Published in final edited form as:
Exp Eye Res. 2009 August ; 89(2): 159–165. doi:10.1016/j.exer.2009.03.002.

Aquaporin-1-facilitated keratocyte migration in cell culture and in vivo corneal wound healing models

Javier Ruiz-Ederra[*] and **A.S. Verkman**[*]
Department of Medicine and Physiology, Cardiovascular Research Institute, 1246 Health Sciences East, University of California, San Francisco, CA 94143-0521, USA

Abstract

Aquaporin-1 (AQP1) water channels are expressed in corneal keratocytes, which become activated and migrate following corneal wounding. The purpose of this study was to investigate the role of AQP1 in keratocyte migration. Keratocyte primary cell cultures from wildtype and AQP1-null mice were compared, as well as keratocyte cultures from pig cornea in which AQP1 expression was modulated by RNAi knockdown and adenovirus-mediated overexpression. AQP1 expression was found in a plasma membrane pattern in corneal stromal and cultured keratocytes. Osmotic water permeability, as measured by calcein fluorescence quenching, was AQP1-dependent in cultured keratocytes, as was keratocyte migration following a scratch wound. Keratocyte migration in vivo was compared in wildtype and AQP1 knockout mice by histology and immunofluorescence of corneal sections at different times after partial-thickness corneal stromal debridement. AQP1 expression in keratocytes was increased by 24 h after corneal debridement. Wound healing and keratocyte appearance near the wound margin were significantly reduced in AQP1 knockout mice, and the number of neutrophils was increased. These results implicate AQP1 water permeability as a new determinant of keratocyte migration in cornea.

Keywords

AQP1; water channel; keratocytes; cornea; wound healing

1. Introduction

Several aquaporin (AQP) type water channels are expressed in the eye, including AQP0 in lens fiber cells, AQP1 in corneal endothelium, keratocytes, ciliary epithelium and lens epithelium, AQP3 in corneal and conjunctival epithelium, AQP4 in ciliary epithelium and retinal Muller cells, and AQP5 in corneal epithelium (reviewed in Takata et al., 2004; King et al., 2004; Verkman et al., 2008). AQP0 deletion or mutation in mice and humans produces cataracts (Berry et al., 2000; Shiels et al., 2001). Evidence from phenotype comparisons in AQP knockout mice suggests AQP involvement in corneal transparency (Thiagarajah and Verkman, 2002), lens transparency (Ruiz-Ederra and Verkman, 2006), regulation of intraocular pressure (Zhang et al., 2002), light signal transduction and retinal edema (Da and Verkman, 2004; Li et al., 2002), and the repair of corneal epithelial wounds (Levin and Verkman, 2006). These functions suggest the possibility of pharmacological

[*]Corresponding authors at: Department of Medicine and Physiology, Cardiovascular Research Institute, 1246 Health Sciences East, University of California, San Francisco, CA 94143-0521, USA. Tel.: +1 415 476 8530; fax: +1 415 665 3847, javiruizederra@yahoo.es (J. Ruiz-Ederra), alan.verkman@ucsf.edu (A.S. Verkman), URL: http://www.ucsf.edu/verklab.

modulation of AQP expression or function in the therapy of glaucoma, cataracts, and corneal and retinal injury. The role of AQP1 in keratocytes is unknown.

The corneal stroma consists of a precisely organized extracellular matrix of collagen fibrils and proteoglycans, including decorin, lumican, keratocan and mimecan, in which is embedded a low density of keratocytes (Meek and Boote, 2004). The functions of keratocytes include generation of the extracellular stromal matrix, and maintenance of corneal transparency and shape (Fini, 1999). Keratocytes normally remain quiescent, but upon injury become stimulated to initiate cell death or to transform into a repair phenotype in which they take on fibroblast-like morphological characteristics including a fusiform shape, multiple nucleoli and absence of cytoplasmic granules, or myofibroblast characteristics, with enlarged size and expression of alpha smooth muscle actin (αSMA) (Fini and Stramer, 2005; West-Mays and Dwivedi, 2006). Migration of keratocytes through the dense corneal stroma is an important process in their response to injury.

Here, we investigated the hypothesis that AQP1 expression in keratocytes facilitates their migration toward a wound. This hypothesis was motivated by our discovery of the involvement of AQPs in cell migration, originally in endothelial cells (Saadoun et al., 2005a), and subsequently in various other cell types (reviewed in Papadopoulos et al., 2008). We proposed that AQPs facilitate cell migration by increasing water permeability at the leading edge of migrating cells, accelerating the formation of lamellipodial protrusions in response to actin depolymerization and ion uptake. We found remarkable impairment in the migration of AQP4-defi-cient glial cells in brain toward a stab wound (Auguste et al., 2007), where glial cells are required to migrate through a dense parenchyma having narrow extracellular spaces, similar to the requirements for migration of keratocytes in corneal stroma. Here, to study AQP1-dependent keratocyte migration, we established keratocyte cell culture models of wound repair and a mouse model of corneal stromal wounding.

2. Material and methods

2.1. Eyes for cell culture and corneal wound studies

Keratocyte cell cultures were generated from murine and porcine corneas. Pig eyes were obtained from Pork Power Farms (Turlock, CA) within few hours after death. Transgenic mice deficient in AQP1 in a CD1 genetic background were generated by targeted gene disruption as described (Ma et al., 1998). All experimental methods and animal care procedures adhered to the ARVO Statement for the Use of Animals in Ophthalmic and Vision Research, and were approved by the University of California, San Francisco Institutional Animal Care and Use Committee (IACUC).

2.2. Keratocyte cell culture

Primary cultures of keratocytes were generated from fresh pig and mouse eyes as described previously for monkey keratocytes, with modifications (Kawakita et al., 2006). Globes were washed in 70% methanol for 2 min followed by 3 washes in sterile HCO_3^--free medium (product 18045–088, Invitrogen, Carlsbad, CA). Under a laminar flow hood, corneas were dissected, taking care to exclude the limbus, and digested in 3 ml dispase II (2.4 U/ml, Roche, Mannheim, Germany) at room temperature while shaking at 140 rpm for 2–3 h. Partially digested corneas from pig were cut in 6–8 pieces and the remaining inner layers (Descemet's membrane, endothelium, Bowman's membrane and epithelium) were mechanically removed with a scalpel (#21, Fisher Scientific, Los Angeles, CA). Partially digested corneas from mice were retained on a 100 μm pore size strainer (Fisher) and inner corneal layers were removed by peeling using two forceps. The remaining corneal stroma (from pig and mice) was incubated for 8–16 h at 37 °C while shaking with DMEM

containing 1 mg/ml collagenase A, 20 mM HEPES (both from Sigma), 50 mg/ml gentamicin, and 1.25 μg/ml amphotericin B (both from Invitrogen) in a 15 ml tube. Afterwards, cells were resuspended in keratinocyte serum-free medium (KSFM, Invitrogen) and seeded at a density of 10^5 cells/cm^2 on collagen type I plates (BD Biosciences, Bedford, MA) at 37 °C under 5% CO_2. Keratocyte morphology was maintained in KSFM medium, but became fibroblast-like upon replacement with DMEM containing 10% FBS (Invitrogen) for 5–7 days. For some experiments pig keratocytes were treated with pig AQP1 siRNA or with AQP4 or Kir4.1 siRNA (negative controls) (Dharmacon, Lafayette, CO) at 80–95% confluence using RNAiMAX transfection reagent (Invitrogen). Transfection efficiency was optimized and confirmed using siGLO transfection fluorescent indicators (Dharmacon), and reduction in AQP1 protein expression was confirmed by immunofluorescence and immunoblot analysis using AQP1 antibody (Chemicon, Temecula, CA). Experiments were done at 48–72 h after transfections. In some experiments pig keratocytes were infected with recombinant adenovirus encoding AQP1 (AQP1-Ad) at 1000 pfu/cell, custom generated by ViraQuest (North Liberty, IA). Experiments were done at 72 h after viral infection.

2.2.1. Osmotic water permeability—Keratocytes were seeded on collagen-coated coverslips and their cytoplasm was labelled with calcein by incubation with 10 μM calcein-AM (Molecular Probes, Eugene, OR) for 30 min at room temperature. Osmotic water permeability was measured from the kinetics of calcein fluorescence in response to changing perfusate osmolalities from 300 (PBS) to 150 mOsm (PBS 1:1 diluted with water), as described (Solenov et al., 2004). Calcein fluorescence was measured using a Nikon TE-2000 inverted fluorescence microscope equipped with 40× objective lens and photomultiplier, amplifier, and analog-to-digital converter. The time course of fluorescence in response to osmotic gradients was fitted to a single exponential function with time constant, τ: $F(t) = A + B\, e^{-t/\tau}$, where A and B are related to system sensitivity and background signal.

2.2.2. In vitro wound healing assay—In vitro wound healing was analyzed in confluent cell monolayers incubated in DMEM containing 10% FBS grown on collagen type I plates (BD Biosciences) as described (Saadoun et al., 2005a). Briefly, cells were scraped in an approximately 300-μm wide strip using a standard 200-μl pipette tip. The wounded monolayers were washed twice to remove non-adherent cells. Phase contrast micrographs at 4× were taken just after cells were scraped and after 24 h. Wound healing was quantified as the area covered by the wound edges over 24 h.

2.2.3. In vivo wound healing—Mice were anesthetized by intraperitoneal injection of 2,2,2-tribromoethanol (avertin, 125 mg/kg; Sigma–Aldrich, St. Louis, MO), and proparacaine (0.5%) was applied to the corneas of both eyes. A previously reported model of epithelial debridement was used with modifications (Stramer et al., 2003; Mohan et al., 1998). Under an operating microscope, the central epithelium was debrided by applying an Alger Brush II (Alger equipment Co., Lago Vista, TX) for 20 s within a 0.5-mm diameter area, which disrupts Bowman's membrane and results in removal of the epithelium and anterior part of the stroma. Buprenorphine (0.1 mg/kg) was administered for pain relief after surgery. Mice were allowed to recover in a heated cage to maintain normothermia. Mice were euthanized by anesthesia and cervical dislocation at 5 min, 24, 48 and 72 h after injury, and eyes were enucleated and fixed in PBS containing 4% paraformaldehyde for at least 4 h at 4 °C. After fixation tissues were processed through graded concentrations of ethanol, followed by Citrisolv (Fisher), and embedded in paraffin. Five serial sagittal sections (5 μm thickness, 10 μm between sections) at the central cornea were cut on a microtome, parallel to the optic nerve. Only eye sections with a proper sagittal orientation were analyzed, using as selection criteria iris aperture and presence of the optic nerve head. At least five mice of each genotype were analyzed at each study time point. H&E-stained corneas were imaged

using a brightfield microscope (Leica, Heidelberg, Germany) equipped with a digital camera (Spot, Sterling Heights, MI). Three fields of ~0.025 cm^2 from the central cornea at 400× total magnification were imaged, located at the site of wound (w), ~50 μm adjacent to the wound (a) and ~1 mm distal to the wound (d). The numbers of keratocytes and polymorphonuclear leukocytes in the 3 regions were determined before and at different times after injury.

2.3. Histology and immunofluorescence

Eye sections were deparaffinized in Citrisolv and rehydrated in graded ethanols. After epitope retrieval with citrate buffer (10 mM sodium citrate, 0.05% Tween 20, pH 6, 30 min, 95–100 °C), sections were blocked with 1% bovine and 5% goat sera and incubated with rabbit anti-AQP1 (1:500; Chemicon, Temecula, CA) or rat anti-mouse neutrophil 7/4 antibody (1:100; AbD Serotec, Raleigh, NC). Primary antibodies were detected with Texas Red goat anti-rabbit and Alexa Fluor 488 goat anti-mouse secondary antibodies (each at 1:200; Molecular Probes). For immunostaining of keratocyte cultures, cells were fixed for 15 min with paraformaldehyde at room temperature, blocked, and immunostained for AQP1 and ALDH (1:50 BD Biosciences, San Jose, CA). Primary antibodies were detected with Texas Red goat anti-rabbit and Alexa Fluor 488 donkey anti-rat secondary antibodies (each at 1:200; Molecular Probes).

2.4. Immunoblot analysis

Keratocyte cultures were scraped from plastic plates and homogenized in 50 mM Tris–HCl; 150 mM NaCl; 1 mM EDTA; 0.25% sodium deoxycholate; 1% protease inhibitor cocktail (2 μg/ml aprotinin, 2 μg/ml pepstatin A, 2 μg/ml leupeptin and 100 μg/ml serine (Sigma), 1% NP40 (Fluka), and 1 mM PMSF (Roche)). Homogenates were centrifuged at 1500*g* for 10 min and the supernatant was loaded onto a 4–12% sodium dodecyl sulfate-polyacrylamide gel (20 μg protein/lane). Proteins were transferred to a polyvinylidene difluoride membrane and incubated with rabbit anti-AQP1 antibody (1:1000), followed by horseradish peroxidase-linked anti-rabbit IgG (1:2000, GE Healthcare, USA), and visualized by enhanced chemiluminescence (Roche Diagnostics, Indianapolis, IN). Protein band densitometry was performed using Scion Image for Macintosh (Scion, Frederick, MD), normalizing to actin immunoreactivity.

2.5. Statistical analysis

Statistical analysis was performed using ANOVA.

3. Results

3.1. AQP1 expression in corneal keratocytes

AQP1 expression in keratocytes was studied by immunofluorescence in corneal sections from wildtype (+/+) and AQP1-null (−/−) mice, and from pig. AQP1 immunofluorescence in mouse corneas in Fig. 1A shows AQP1 protein expression (red) in the plasma membrane of corneal endothelial cells and stromal keratocytes. The keratocytes appear as elongated cells with their major axis parallel to stromal fibers. As expected, AQP1 expression was absent in corneas from AQP1-null mice. Fig. 1B shows a similar pattern of AQP1 immunofluorescence in endothelial cells and stromal keratocytes in the substantially thicker pig cornea. These results are in agreement with prior AQP1 immunolocalization studies in corneas from rat (Bondy et al., 1993), cow (Li et al., 1999) and humans (Macnamara et al., 2004).

3.2. AQP1 accelerates cell migration in keratocyte cell cultures

Cell culture conditions were optimized, based on prior reports (Kawakita et al., 2006), to obtain nearly pure keratocyte cultures from mouse and pig corneas. The culture method involved two consecutive enzymatic digestions followed by mechanical removal of the external (non-stromal) corneal layers. The cultures showed little or no contamination by corneal epithelial or endothelial cells as shown by immunocytochemistry (>98% of cells positive for the keratocyte marker ALDH; <5% cells positive for the epithelial cell marker AQP5, not shown) and by phase contrast microscopy (characteristic dendritic shape). AQP1 protein was expressed in a plasma pattern in nearly all cells in keratocyte cultures from mouse and pig corneas (Fig. 2A and B, left panels). AQP1 immunofluorescence was absent in cells cultured from AQP1-null mice, and greatly reduced in cultures from pig cornea after AQP1-RNAi treatment. AQP1 immunoblot analysis of homogenates from wild-type mouse and pig cell cultures showed a prominent band at ~28 kDa (Fig. 2A and B, right panels), which was absent in keratocytes from AQP1-null mice and reduced by ~80% in AQP1-RNAi-treated keratocytes from pig.

Reduced osmotic water permeability was found in AQP1-RNAi-treated keratocytes, as measured using a calcein fluorescence quenching method in which cytoplasmic calcein fluorescence provides a measure of cell volume changes in response to osmotic challenge. Fig. 2C (left) shows representative kinetics of reversible cell swelling in response to serial perfusion with 300 and 150 mOsm PBS. Osmotic equilibration was significantly slowed by 1.7-fold in AQP1-RNAi-treated keratocytes, with a τ^{-1} of 0.30 ± 0.025 s^{-1} (control) vs. 0.18 ± 0.007 s^{-1} (AQP1-RNAi) (Fig. 2C, right).

In vitro analysis of keratocyte migration was performed in near-confluent monolayers of keratocyte cells, which become fibroblast-like after 5–7 days of incubation with DMEM containing 10% FBS. An ~300-μm wide strip of cells was scrapped with a pipette tip, and closure of the ‘wound’ was measured at 24 h. Fig. 2D (left) shows representative micrographs with slowing of wound closure in AQP1-null mouse fibroblasts and RNAi knockdown pig fibroblasts, and acceleration of wound closure in AQP1-Ad-treated pig fibroblasts that overexpressed AQP1. As summarized in Fig. 2D (right), on average there was 2.2-fold slowed wound closure in AQP1-null vs. wildtype mouse fibroblasts, and 1.8-fold slowed wound closure in RNAi knockdown vs. control pig fibroblasts, and 1.3-fold accelerated wound closure in AQP1-Ad-treated pig fibroblasts.

3.3. Delayed healing of debrided corneas in AQP1-null mice

A partial-thickness corneal debridement model was developed to test whether the appearance/migration of keratocytes in AQP1-null corneas is impaired following wounding. After creation of a partial-thickness corneal wound by stromal debridement, paraffin sections from central corneas were analyzed just after wounding, and after 24, 48, and 72 h. Keratocytes were identified by their lack of staining by a neutrophil-specific antibody, which was confirmed in wildtype mice by AQP1 immunostaining. Fig. 3A shows hematoxylin and eosin staining (left panels), neutrophil immunofluorescence (center panels, green) and AQP1 immunofluorescence (right panels, red) in corneal sections from wildtype and AQP1-null mice. Non-wounded corneas in the top left panel show relatively thinner corneas in AQP1-null mice, as reported previously (Thiagarajah and Verkman, 2002). AQP1 is seen in endothelial cells and stromal keratocytes in corneas from wildtype mice. No immunostaining for neutrophils was seen in non-wounded corneas. Just after wounding (panel labelled ‘5 min after wound’), the number of keratocytes was similar to that in undamaged corneas, with no immunostaining for neutrophils detected.

At 24 h after injury, there was increased cellularity in the region of the wound, particularly in corneas from wildtype mice. In addition to keratocytes, neutrophils were present in the cornea, with greatest abundance near the wound, and in corneas from AQP1-null mice. At 24 h after injury, AQP1 became strongly expressed in keratocytes. At 48 h after injury the number of keratocytes in the wound area was reduced to near baseline levels. Neutrophils remained present and were more abundant in corneas from AQP1-null mice. Also, as seen at 24 h, the repair of the corneal wound appeared to be less complete in the AQP1-null mice.

The numbers of keratocytes and neutrophils were counted on a series of micrographs from multiple non-wounded mice and mice wounded at different time points. Fig. 4A shows a schematic of a wounded mouse cornea in which the three boxes represent the regions where micrographs were analyzed: the wounded region (w), an adjacent region (a), and a region far from the site of injury (d).

Fig. 4B shows an increased number of keratocytes at 24 h in the wound area in corneas from wildtype mice, compared to non-injured corneas. The reduced number of keratocytes in corneas from AQP1-null mice at 24 h could represent impaired keratocyte migration and/or increased keratocyte apoptosis. In AQP1-null wounded corneas the maximum number of keratocytes in the wound area was seen at 48 h rather than at 24 h. Interestingly, there was a greater number of neutrophils in corneas from AQP1-null mice at 48 and 72 h in the wound and the adjacent/distal areas (Fig. 4C), which may be a secondary response related to slowed stromal healing in AQP1-null corneas.

4. Discussion

Our results establish AQP1 as a new determinant of keratocyte function. AQP1 knockout or knockdown in primary cultures of keratocytes reduced their migration in an in vitro wound healing assay. In vivo, keratocyte AQP1 protein expression increased after wounding, and keratocyte migration toward a partial-thickness corneal wound appeared to be reduced in AQP1 knockout mice. The slowed healing of stromal wounds in AQP1 deficiency may be a consequence of impaired keratocyte migration.

Impaired migration of AQP1-deficient keratocytes supports the generality of AQP-facilitated cell migration seen in many cell types. AQP1 deficiency impairs endothelial cell migration, resulting in impaired angiogenesis and slowed growth of implanted tumors (Saadoun et al., 2005a). Accelerated migration of AQP-expressing tumor cells increases their local invasiveness and extravasation across blood vessels, increasing their metastatic potential (Hu and Verkman, 2006). AQP-facilitated cell migration is also involved in wound healing, as has been demonstrated for AQP3 in cutaneous (Hara-Chikuma and Verkman, 2008) and corneal (Levin and Verkman, 2004) wounds. Studies of lamellipodial dynamics, polarized AQP expression and osmotic effects suggest that AQP-facilitated water influx into lamellipodia at the leading edge of migrating cells is the responsible factor for increased migration (Saadoun et al., 2005a,b). AQP-facilitated changes in cell volume as cells squeeze through narrow extracellular spaces may also contribute to AQP-dependent cell migration. Indeed, marked impairment was found in the migration of AQP4-deficient glial cells toward a stab injury in brain (Auguste et al., 2007), which may be related to their inability to squeeze through the narrow gaps between brain cells. The impairment in migration of AQP1-deficient keratocytes may involve a similar mechanism, since keratocytes in the injured cornea migrate toward a chemotactic stimulus through the dense stromal matrix.

Together with the delayed appearance of keratocytes in corneal stroma from AQP1-null mice at 24 h after injury, we found greater neutrophil influx into the wound and adjacent/distal areas at 48 and 72 h. As mentioned in the Introduction, keratocyte functions include

the synthesis and maintenance of stromal extracellular matrix and the maintenance of corneal transparency and shape (Fini,1999). The characteristic dendritic morphology of quiescent keratocytes changes to a fusiform, fibroblast-/myofibroblast-like morphology after injury, which may represent an adaptation to facilitate keratocyte migration through a densely packed network of collagen fibers and other extracellular matrix components (Meek and Boote, 2004; West-Mays and Dwivedi, 2006). It has also been proposed that keratocytes provide a 'cellular highway' for leukocyte trafficking (Burns et al., 2005). A recent paper reported that migrating neutrophils from limbal vessels develop close contacts with keratocytes, with transmission electron microscopy showing 40% of the neutrophil surface in contact with keratocytes following corneal abrasion (Petrescu et al., 2007). The greater and delayed neutrophil response in AQP1-deficient corneas may be related to this phenomenon, as well as to the impaired stromal healing response.

We also found delayed corneal epithelial wound repair in AQP1-null mice by 24 h after injury. During corneal wound healing fibroblasts are major source of hepatocyte growth factor (HGF), which stimulates proliferation of corneal epithelial cells (Wilson et al., 2001; Klenkler and Sheardown, 2004). Therefore, the relatively fewer keratocytes near the wound area in the corneas from AQP1-null mice might reduce the local concentration of HGF. The delayed epithelial repair in AQP1-null corneas might secondarily affect keratocyte migration, as some cytokines released from the injured epithelium have been reported to bind to receptors on keratocytes (Wilson et al., 2001). Notwithstanding our inability to define the precise factor(s) responsible for the in vivo corneal wound phenotype in AQP1 deficiency, our results indicate AQP1 as an important determinant in corneal stromal wound repair.

AQP1-dependent keratocyte migration adds to an expanding list of cell types whose migration is increased by AQP-facilitated water permeability, which, in the eye, includes AQP3-facilitated migration of corneal epithelial cells (Levin and Verkman, 2006). AQP1-facilitated angiogenesis in retinopathies is another possible ocular manifestation of this paradigm; however, we found little AQP1 protein expression in microvessels in a neonatal mouse model of oxygen-deprivation retinopathy, and unimpaired retinal angiogenesis in AQP1-deficient mice (Ruiz-Ederra and Verkman, 2007). Our results here suggest the possibility of drug modulation of keratocyte AQP1 expression to control one aspect of the response of the corneal stroma to acute and chronic injury, which may be of relevance, for example, in treatment of complications of refractive surgery.

Acknowledgments

This work was supported by grants EY13574, DK35124, HL59198, EB00415, DK72517 and HL73856. The authors thank Liman Qian for mouse breeding and genotype analysis and Dr. Marc Levin for suggesting the possibility of AQP1-dependent keratocyte migration and for helpful advice.

References

Auguste KI, Jin S, Uchida K, Yan D, Manley GT, Papadopoulos MC, Verkman AS. Greatly impaired migration of implanted aquaporin-4-deficient astroglial cells in mouse brain toward a site of injury. FASEB J. 2007; 21:108–116. [PubMed: 17135365]

Berry V, Francis P, Kaushal S, Moore A, Bhattacharya S. Missense mutations in MIP underlie autosomal dominant 'polymorphic' and lamellar cataracts linked to 12q. Nat Genet. 2000; 25:15–17. [PubMed: 10802646]

Bondy C, Chin E, Smith BL, Preston GM, Agre P. Developmental gene expression and tissue distribution of the CHIP28 water-channel protein. Proc Natl Acad Sci USA. 1993; 90:4500–4504. [PubMed: 8506291]

Burns AR, Li Z, Smith CW. Neutrophil migration in the wounded cornea: the role of the keratocyte. Ocul Surf. 2005; 3:S173–S176. [PubMed: 17216113]

Da T, Verkman AS. Aquaporin-4 gene disruption in mice protects against impaired retinal function and cell death after ischemia. Invest Ophthalmol Vis Sci. 2004; 45:4477–4483. [PubMed: 15557457]

Fini ME. Keratocyte and fibroblast phenotypes in the repairing cornea. Prog Retin Eye Res. 1999; 18:529–551. [PubMed: 10217482]

Fini ME, Stramer BM. How the cornea heals: cornea-specific repair mechanisms affecting surgical outcomes. Cornea. 2005; 24:S2–S11. [PubMed: 16227819]

Hara-Chikuma M, Verkman AS. Prevention of skin tumorigenesis and impairment of epidermal cell proliferation by targeted aquaporin-3 gene disruption. Mol Cell Biol. 2008; 28:326–332. [PubMed: 17967887]

Hu J, Verkman AS. Increased migration and metastatic potential of tumor cells expressing aquaporin water channels. FASEB J. 2006; 20:1892–1894. [PubMed: 16818469]

Kawakita T, Espana EM, He H, Smiddy R, Parel JM, Liu CY, Tseng SC. Preservation and expansion of the primate keratocyte phenotype by down-regulating TGF-beta signaling in a low-calcium, serum-free medium. Invest Ophthalmol Vis Sci. 2006; 47:1918–1927. [PubMed: 16638999]

King LS, Kozono D, Agre P. From structure to disease: the evolving tale of aquaporin biology. Nat Rev Mol Cell Biol. 2004; 5:687–698. [PubMed: 15340377]

Klenkler B, Sheardown H. Growth factors in the anterior segment: role in tissue maintenance, wound healing and ocular pathology. Exp Eye Res. 2004; 79:677–688. [PubMed: 15500826]

Levin MH, Verkman AS. Aquaporin-dependent water permeation at the mouse ocular surface: in vivo microfluorimetric measurements in cornea and conjunctiva. Invest Ophthalmol Vis Sci. 2004; 45:4423–4432. [PubMed: 15557451]

Levin MH, Verkman AS. Aquaporin-3-dependent cell migration and proliferation during corneal re-epithelialization. Invest Ophthalmol Vis Sci. 2006; 47:4365–4372. [PubMed: 17003427]

Li J, Kuang K, Nielsen S, Fischbarg J. Molecular identification and immunolocalization of the water channel protein aquaporin 1 in CBCECs. Invest Ophthalmol Vis Sci. 1999; 40:1288–1292. [PubMed: 10235568]

Li J, Patil RV, Verkman AS. Mildly abnormal retinal function in transgenic mice without Muller cell aquaporin-4 water channels. Invest Ophthalmol Vis Sci. 2002; 43:573–579. [PubMed: 11818406]

Ma T, Yang B, Gillespie A, Carlson EJ, Epstein CJ, Verkman AS. Severely impaired urinary concentrating ability in transgenic mice lacking aquaporin-1 water channels. J Biol Chem. 1998; 273:4296–4299. [PubMed: 9468475]

Macnamara E, Sams GW, Smith K, Ambati J, Singh N, Ambati BK. Aquaporin-1 expression is decreased in human and mouse corneal endothelial dysfunction. Mol Vis. 2004; 10:51–56. [PubMed: 14758337]

Meek KM, Boote C. The organization of collagen in the corneal stroma. Exp Eye Res. 2004; 78:503–512. [PubMed: 15106929]

Mohan R, Rinehart WB, Bargagna-Mohan P, Fini ME. Gelatinase B/lacZ transgenic mice, a model for mapping gelatinase B expression during developmental and injury-related tissue remodeling. J Biol Chem. 1998; 273:25903–25914. [PubMed: 9748266]

Papadopoulos MC, Saadoun S, Verkman AS. Aquaporins and cell migration. Pflugers Arch. 2008; 456:693–700. [PubMed: 17968585]

Petrescu MS, Larry CL, Bowden RA, Williams GW, Gagen D, Li Z, Smith CW, Burns AR. Neutrophil interactions with keratocytes during corneal epithelial wound healing: a role for CD18 integrins. Invest Ophthalmol Vis Sci. 2007; 48:5023–5029. [PubMed: 17962453]

Ruiz-Ederra J, Verkman AS. Accelerated cataract formation and reduced lens epithelial water permeability in aquaporin-1-deficient mice. Invest Ophthalmol Vis Sci. 2006; 47:3960–3967. [PubMed: 16936111]

Ruiz-Ederra J, Verkman AS. Aquaporin-1 independent microvessel proliferation in a neonatal mouse model of oxygen-induced retinopathy. Invest Ophthalmol Vis Sci. 2007; 48:4802–4810. [PubMed: 17898307]

Saadoun S, Papadopoulos MC, Hara-Chikuma M, Verkman AS. Impairment of angiogenesis and cell migration by targeted aquaporin-1 gene disruption. Nature. 2005a; 434:786–792. [PubMed: 15815633]

Saadoun S, Papadopoulos MC, Watanabe H, Yan D, Manley GT, Verkman AS. Involvement of aquaporin-4 in astroglial cell migration and glial scar formation. J Cell Sci. 2005b; 118:5691–5698. [PubMed: 16303850]

Shiels A, Bassnett S, Varadaraj K, Mathias R, Al-Ghoul K, Kuszak J, Donoviel D, Lilleberg S, Friedrich G, Zambrowicz B. Optical dysfunction of the crystalline lens in aquaporin-0-deficient mice. Physiol Genomics. 2001; 7:179–186. [PubMed: 11773604]

Solenov E, Watanabe H, Manley GT, Verkman AS. Sevenfold-reduced osmotic water permeability in primary astrocyte cultures from AQP-4-deficient mice, measured by a fluorescence quenching method. Am J Physiol. 2004; 286:C426–C432.

Stramer BM, Zieske JD, Jung JC, Austin JS, Fini ME. Molecular mechanisms controlling the fibrotic repair phenotype in cornea: implications for surgical outcomes. Invest Ophthalmol Vis Sci. 2003; 44:4237–4246. [PubMed: 14507867]

Takata K, Matsuzaki T, Tajika Y. Aquaporins: water channel proteins of the cell membrane. Prog Histochem Cytochem. 2004; 39:1–83. [PubMed: 15242101]

Thiagarajah JR, Verkman AS. Aquaporin deletion in mice reduces corneal water permeability and delays restoration of transparency after swelling. J Biol Chem. 2002; 277:19139–19144. [PubMed: 11891232]

Verkman AS, Ruiz-Ederra J, Levin MH. Functions of aquaporins in the eye. Prog Retin Eye Res. 2008; 27:420–433. [PubMed: 18501660]

West-Mays JA, Dwivedi DJ. The keratocyte: corneal stromal cell with variable repair phenotypes. Int J Biochem Cell Biol. 2006; 38:1625–1631. [PubMed: 16675284]

Wilson SE, Mohan RR, Mohan RR, Ambrósio R Jr, Hong J, Lee J. The corneal wound healing response: cytokine-mediated interaction of the epithelium, stroma, and inflammatory cells. Prog Retin Eye Res. 2001; 20:625–637. [PubMed: 11470453]

Zhang D, Vetrivel L, Verkman AS. Aquaporin deletion in mice reduces intraocular pressure and aqueous fluid production. J Gen Physiol. 2002; 119:561–569. [PubMed: 12034763]

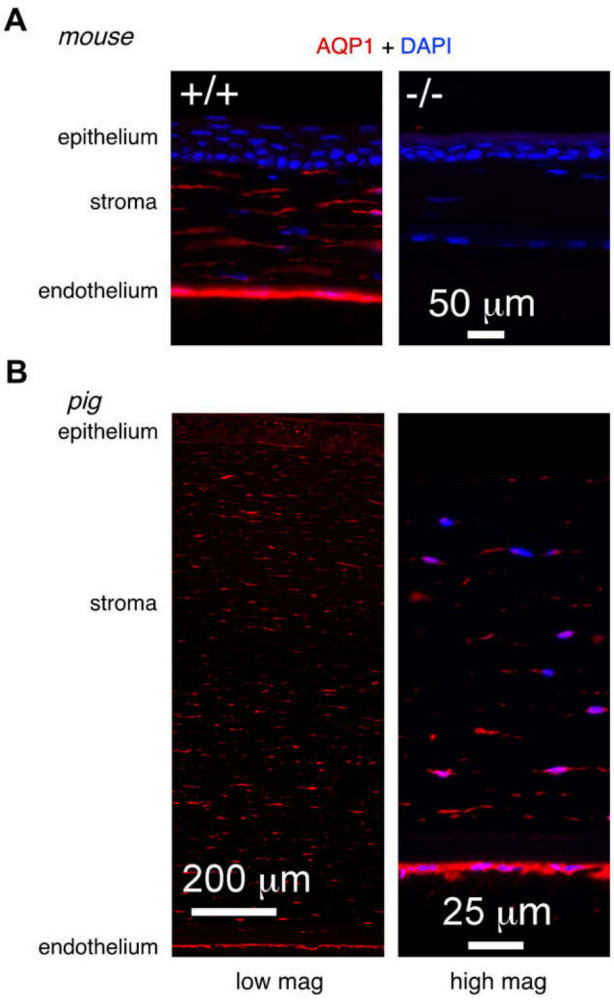

Fig. 1.

AQP1 expression in mouse and pig cornea. (A) AQP1 immunofluorescence in corneas from wildtype (+/+) (left) and AQP1 knockout (−/−) (right) mice. (B) AQP1 immunofluorescence in pig corneas shown at low (left) and high (right) magnification. Nuclei stained blue with DAPI. (For interpretation of the references to colour in this figure legend, the reader is referred to the web version of this article.)

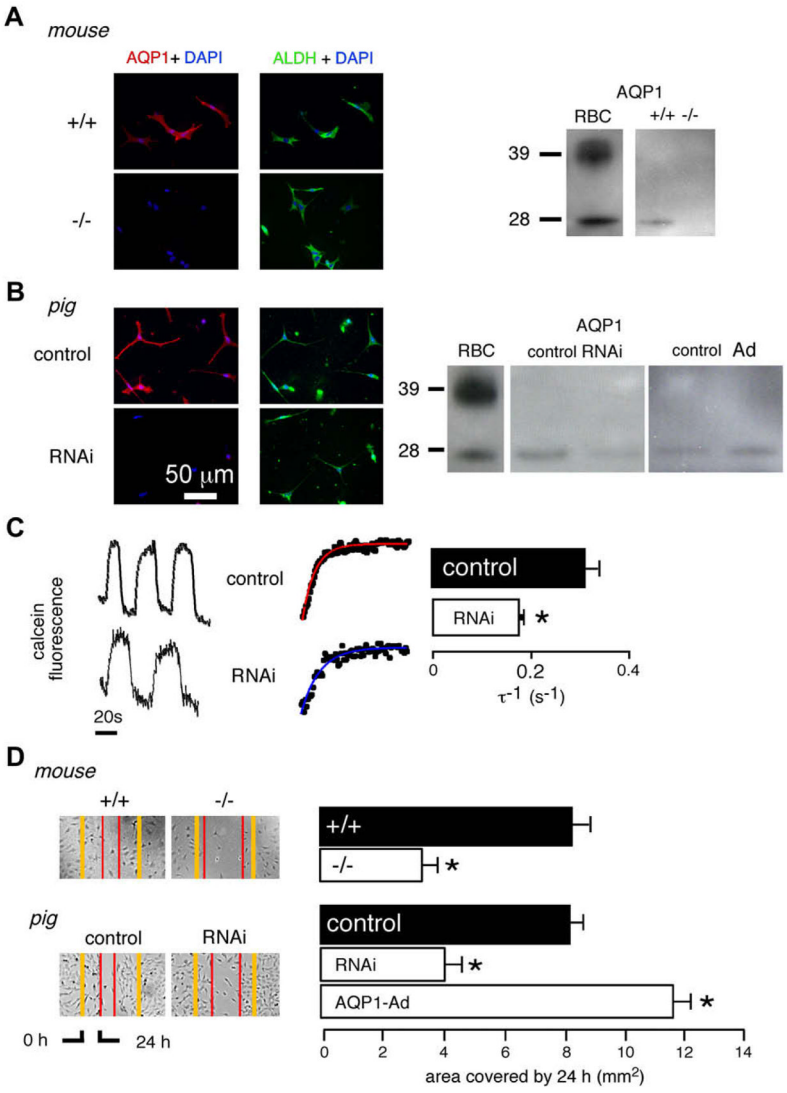

Fig. 2.

Cell migration in keratocyte cultures. (A) (Left) AQP1 (red) and ALDH (green) immunofluorescence in keratocyte cultures from wildtype mice (+/+) and AQP1 knockout (−/−) mice. Nuclei stained blue with DAPI. (Right) AQP1 immunoblot analysis. (B) (Left) AQP1 (red) and ALDH (green) immunofluorescence in control and AQP1-RNAi-treated keratocyte cultures from pig. (Right) AQP1 immunoblot analysis. Mouse and pig blood cell (RBC) membranes used as positive controls. (C) Osmotic water permeability. (Left) Representative calcein fluorescence recordings in response to hypoosmolar challenge. Expanded view with exponential fits shown in middle panel. Perfusate switch from PBS to PBS:water (1:1) results in osmotic cell swelling and increased calcein fluorescence. (Right) Reciprocal exponential time constants for osmotic equilibration (τ^{-1}) from control and AQP1-RNAi-treated pig keratocyte cultures (SE, $n = 4$, $^*p < 0.01$). (D) In vitro wound healing assay. (Left) Phase contrast micrographs of wounded cell monolayers showing wound closure at 24 h in mouse and pig keratocyte cell cultures. (Right) Summary of wound closure data (SE, $n = 4$, $^*p < 0.01$). (For interpretation of the references to colour in this figure legend, the reader is referred to the web version of this article.)

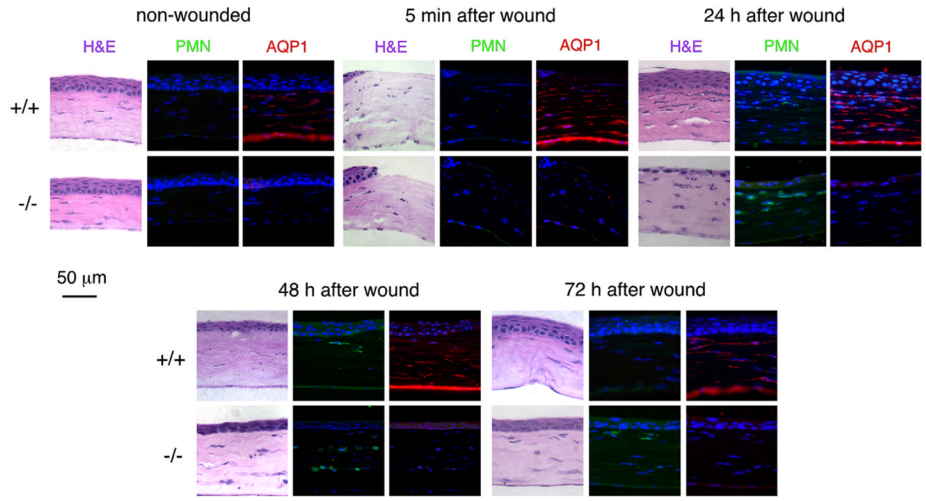

Fig. 3.

Healing of partial-thickness corneal stromal wounds in mice. H&E, neutrophils (green) and AQP1 (red) stained section from central mouse corneas. Nuclei stained with DAPI (blue). Micrographs shown for non-wounded corneas and at indicated times after wounding. (For interpretation of the references to colour in this figure legend, the reader is referred to the web version of this article.)

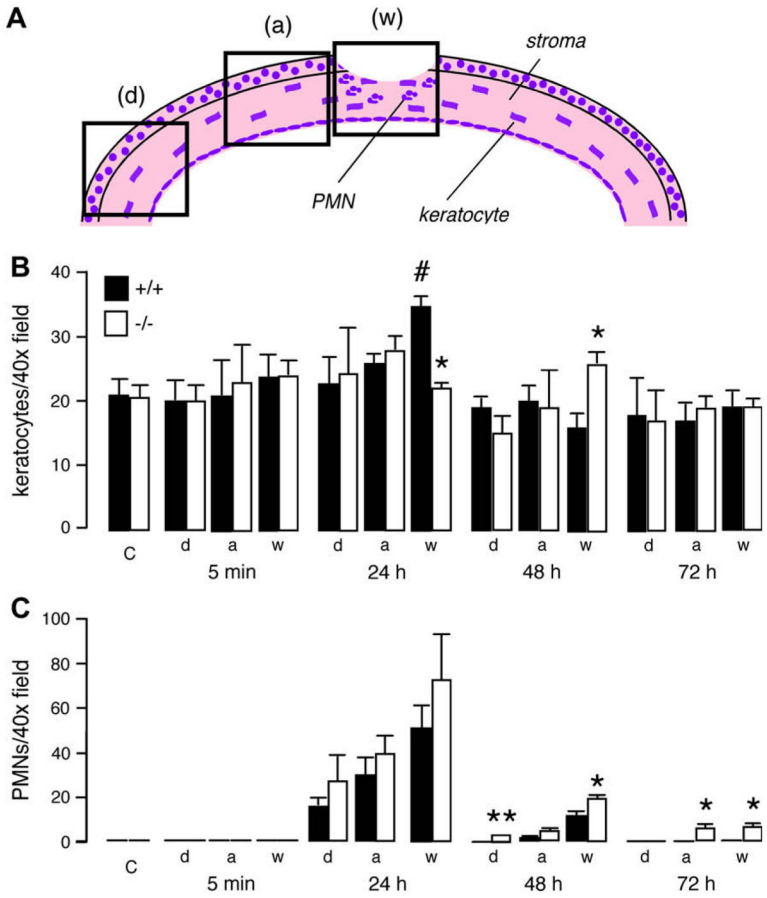

Fig. 4.

Quantification of corneal wound healing. (A) Diagram showing areas of mouse corneas analyzed. (B) Number of keratocytes per 40× (total magnification 400×) field, and (C) number of neutrophils per 40× field (SE, $n = 5$, *: compared to wildtype, $p < 0.05$; #: compared to control non-injured corneas, $p < 0.01$); a: adjacent region; d: distal region; w: wounded region; C: non-wounded cornea.